NANO LETTERS

2003
Vol. 3, No. 8
1167−1171

Electrospinning of Polymeric and Ceramic Nanofibers as Uniaxially Aligned Arrays

Dan Li, Yuliang Wang, and Younan Xia*

Department of Chemistry, University of Washington, Seattle, Washington 98195

Received June 20, 2003

ABSTRACT

Electrospinning has been applied to prepare uniaxially aligned nanofibers made of organic polymers, ceramics, and polymer/ceramic composites. The key to the success of this method was the use of a collector consisting of two pieces of electrically conductive substrates separated by a gap whose width could be varied from hundreds of micrometers to several centimeters. As driven by electrostatic interactions, the charged nanofibers were stretched to span across the gap and thus to become uniaxially aligned arrays over large areas. Because the nanofibers were suspended over the gap, they could be conveniently transferred onto the surfaces of other substrates for subsequent treatments and various applications. Materials that have been successfully incorporated into this procedure include conventional organic polymers, graphite carbon, and metal oxides. By controlling the parameters for electrospinning, we have also fabricated a number of simple device structures, for example, an individual nanofiber spanning across two electrodes, 2D arrays of crossbar junctions, and optical polarizers.

Electrospinning has been extensively explored as a simple and versatile method for drawing fibers from polymer solutions (or melts).[1] In a typical process, the polymeric fluid is extruded from the orifice of a needle to form a small droplet in the presence of an electric field. When the electric field is sufficiently strong, charges built up on the surface of the droplet will overcome the surface tension to induce the formation of a liquid jet that is subsequently accelerated toward a grounded collector. As the solvent is evaporating, this liquid jet is stretched to many times its original length to produce continuous, ultrathin fibers of the polymer.[2] In the continuous feeding mode (through the use of a syringe pump), many copies of ultrathin fibers can be obtained within a relatively short period of time. In the past several decades, this technique has been successfully exploited to generate thin fibers from a broad range of polymers, with typical examples including engineering plastics, biopolymers, conducting polymers, block copolymers, and polymer blends.[3] More recently, it has also been extended to fabricate nanofibers made of ceramics and composite materials.[4] As limited by the chaotic motion (or bending instability) of the highly charged jet, the electrospun fibers are often collected as randomly oriented structures in the form of nonwoven mats. Although these mats are of great interest for applications that include texturing, composite reinforcement, membrane-based separation, sensing, enzyme immobilization, and tissue engineering,[5] their disordered structures seem to be problematic for use with device fabrications (in, for example, microelectronics and photonics) that often require well-aligned and highly ordered architectures.[6]

The challenge of controlling the spatial orientation of electrospun fibers has been met with some success. Both mechanical and electrostatic means have been explored to improve the alignment of electrospun nanofibers. Reneker et al. have shown that the as-spun fibers could be aligned more or less parallel to each other when a drum rotating at high speed was used as the collector.[7] Zussman et al. have demonstrated the use of a wheel-like bobbin as the collector to position and align individual polymer nanofibers into parallel arrays.[8] Because the edge of such a bobbin had to be relatively sharp, this technique does not seem to be feasible for forming well-aligned nanofibers over large areas. Deitzel et al. have obtained yarns of aligned poly(ethylene oxide) fibers by introducing an electrostatic lens element to stabilize the liquid jet.[9] Vaia et al. have fabricated aligned yarns of nylon-6 nanofibers by rapidly oscillating a grounded frame within the jet, but no detailed description and discussion were provided in their publication.[10] The degree of alignment that they could achieve and the areas of their samples were also not clear. More recently, Wendorff et al. reported the use of a metal frame as the collector to generate parallel arrays of polyamide nanofibers with an average diameter of 50 nm.[11] Here we report a simple and versatile method that generated uniaxially aligned nanofibers over large areas by introducing a gap into the conventional collector. As assisted by electrostatic interactions, the nanofibers were stretched across the gap to form a parallel array,

* Corresponding author. E-mail: xia@chem.washington.edu.

10.1021/nl0344256 CCC: $25.00
Published on Web 07/08/2003

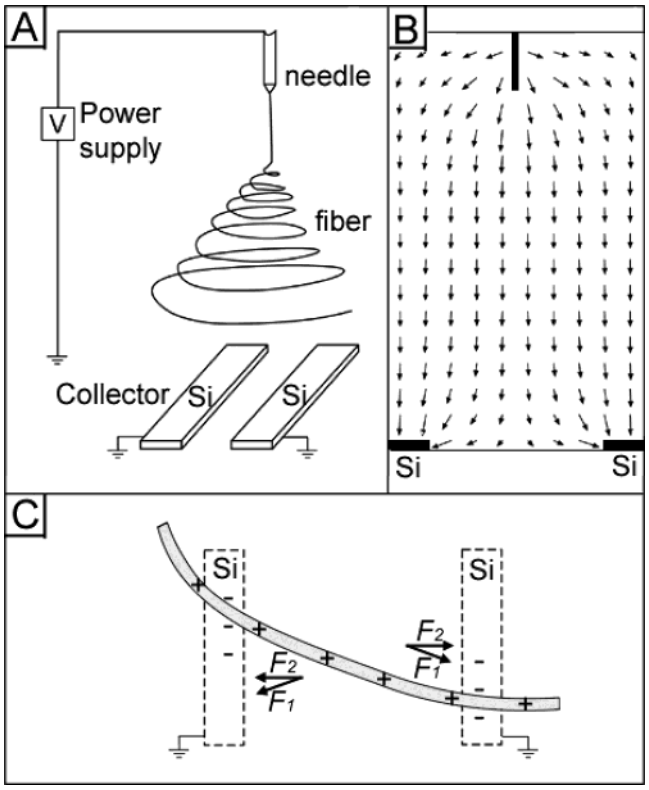

Figure 1. (A) Schematic illustration of the setup for electrospinning that we used to generate uniaxially aligned nanofibers. The collector contained two pieces of conductive silicon stripes separated by a gap. (B) Calculated electric field strength vectors in the region between the needle and the collector. The arrows denote the direction of the electrostatic field lines. (C) Electrostatic force analysis of a charged nanofiber spanning across the gap. The electrostatic force (F_1) resulted from the electric field and the Coulomb interactions (F_2) between the positive charges on the nanofiber and the negative image charges on the two grounded electrodes.

which could be conveniently transferred onto the surface of another substrate for various applications.

Figure 1A illustrates the schematic setup used for our electrospinning experiments. It is essentially the same as the conventional configuration[1] except for the use of a collector containing a gap in its middle. Such a collector could be simply fabricated by putting two stripes of electrical conductors (e.g., metals and highly doped silicon) together or by cutting a piece of aluminum foil. The width of the gap could be varied from hundreds of micrometers to several centimeters. Figure 1B shows a cross-sectional view of the electric field strength vectors between the needle and the grounded collector calculated using the Student's QuickField program. Unlike the conventional system, the electric field lines in the vicinity of the collector were split into two fractions pointing toward opposite edges of the gap. Figure 1C illustrates the electrostatic forces acting on a charged nanofiber spanning the gap. The as-spun fiber can be considered to be a string of positively charged elements connected through a viscoelastic medium. In general, the charged nanofiber should experience two sets of electrostatic forces: the first set (F_1) originating from the splitting electric field and the second one between the charged fiber and image charges induced on the surfaces of the two grounded electrodes (F_2). In particular, electrostatic force F_1 should be in the same direction as the electric field lines and should pull the two ends of the fiber toward the two electrodes. Once the charged fiber has moved into the vicinity of the electrodes, charges on the fiber will induce opposite charges on the surfaces of the electrodes. Considering that Coulomb interactions are inversely proportional to the square of the separation between charges, the two ends of the fiber closest to the electrodes should generate the strongest electrostatic force (F_2), which will stretch the nanofiber across the gap to have it positioned perpendicular to the edge of the electrode. In addition, unlike fibers directly deposited on top of an electrode where they can be immediately discharged, the fibers suspended across the gap can remain highly charged after deposition. The electrostatic repulsion between the deposited and the upcoming fibers can further enhance the parallel alignment (because it represents the lowest-energy configuration for an array system of highly charged fibers).

In a typical procedure, a polymer solution was loaded into a plastic syringe equipped with a 23 gauge needle made of stainless steel. The needle was connected to a high-voltage supply (ES30P-5W, Gamma High Voltage Research Inc., Ormond Beach, FL) that is capable of generating DC voltages up to 30 kV. The solution was continuously supplied using a syringe pump (KDS-200, Stoelting, Wood Dale, IL) at a rate of 0.2 mL/h for poly(vinyl pyrrolidone) (PVP) solutions and 0.3 mL/h for polyacrylonitrile (PAN) solutions. A voltage of 5 kV was applied for electrospinning. The distance between the needle tip and the collector was 7.6 cm when PVP solutions were electrospun and 14 cm for PAN solutions. SEM images were taken using a field-emission scanning electron microscope (Sirion, FEI, Portland, OR) operated at an accelerating voltage of 5 kV, and the samples were not coated with any conductive layers before imaging. The diameters of these fibers were quantitatively measured from their high-magnification SEM images. The Rayleigh scattering spectra were obtained using an optical fiber spectrometer (Ocean Optics, S2000; the beam spot was ~5 mm^2 in area).

Our initial demonstrations involved the use of PVP with an average molecular weight around 1 300 000 g/mol. Figure 2A shows a typical optical micrograph of PVP nanofibers that were electrospun from a solution containing 0.5 g of PVP and 4.2 mg of tetramethylammonium chloride in a mixture of 8 mL of ethanol and 4 mL of water and collected over a gap formed between two stripes of silicon substrates. Panels B and C of Figure 2 show SEM images of the same sample, displaying nanofibers deposited across the gap and on top of the silicon stripe, respectively. These images clearly indicate that the polymer nanofibers were uniaxially aligned across the gap with their longitudinal axes oriented perpendicular to the edges of the gap. In comparison, the nanofibers directly deposited on top of the silicon stripe (Figure 2C) were essentially disordered in spatial orientation. Figure 2D shows the SEM image of another sample that was taken from a region close to the edge of the silicon stripe. These

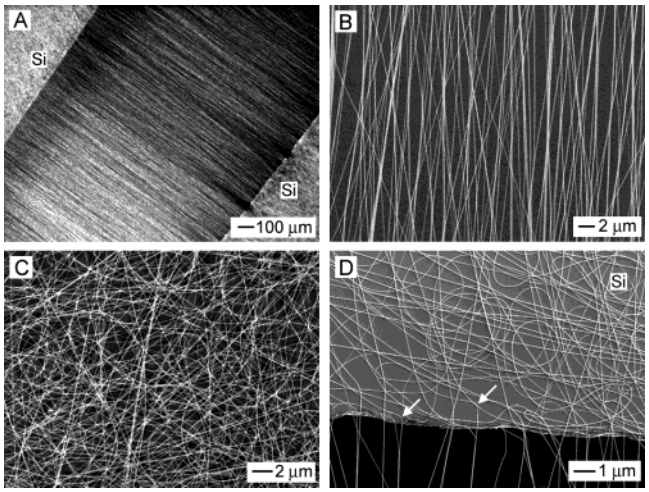

Figure 2. Images showing the orientation of PVP nanofibers on a collector containing a gap in its middle. (A) Dark-field optical micrograph of PVP nanofibers collected on top of a gap formed between two silicon stripes. (B, C) SEM images taken from the same sample, showing nanofibers deposited (B) across the gap and (C) on top of the silicon stripe. (D) SEM image of another sample taken from a region close to the edge of the gap.

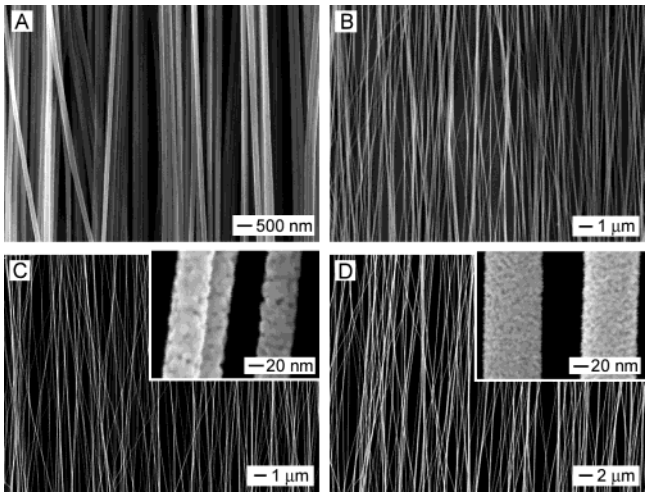

Figure 3. SEM image of uniaxially aligned nanofibers made of various materials: (A) carbon nanofibers, (B) TiO_2/PVP, (C) TiO_2, and (D) Sb-doped SnO_2. The insets show enlarged SEM images of these ceramic nanofibers.

nanofibers were collected within a shorter period of time (5 s versus 2 min) so that any change in spatial orientation could be clearly identified. It is interesting that some nanofibers took sharp turns (as indicated by arrows) to position themselves perpendicular to the edge of the silicon stripe as they were about to enter the gap. Such a dramatic change in spatial orientation strongly supports the action of electrostatic forces illustrated in Figure 1.

Using this simple setup, PVP nanofibers with diameters ranging from tens of nanometers to several micrometers have been prepared as uniaxially aligned arrays by fine-tuning the conditions for electrospinning. The stacking density of these nanofibers was found to depend on a number of parameters that include the width of the gap and the collection time. Narrower gaps and longer collection times both led to the formation of denser arrays. The arrayed nanofibers could be easily transferred to the surface of another substrate by vertically moving this substrate through the gap. When gaps of >1 cm across were used to collect nanofibers thinner than 150 nm in diameter, the aligned nanofibers tended to be broken during the spinning process because these fibers were not sufficiently strong to support their own weight, as well as the electrostatic repulsions applied by other charged fibers. In these cases, nongrounded substrates (e.g., glass slides, polymer plates, or silicon wafers) could be placed within the gap to help support the nanofibers. These additional substrates had essentially no influence on the quality (degree of alignment and size) of resultant nanofibers. By this means, we have fabricated uniaxially aligned nanofibers up to several centimeters in length. These nanofibers could also be transferred to other substrates for subsequent treatments and applications.

This procedure has also been extended to generate uniaxially aligned nanofibers from a rich variety of polymers other than PVP, with typical examples including poly(ethylene oxide), polystyrene, and polyacrylonitrile. Figure 3A shows the SEM image of a parallel array of carbon nanofibers that were electrospun from a 10 wt % polyacrylonitrile solution in dimethylformamide using a spinning voltage of 9 kV, followed by stabilization (in air) at 270 °C for 15 min and carbonization under argon at 800 °C for 1 h.[12] After carbonization at 800 °C for 1 h, the average diameter of these fibers was reduced from 420 to 170 nm. Our electron diffraction studies indicated that carbon nanofibers obtained at this temperature had an amorphous structure. In addition to pure polymers, we found that nanofibers consisting of inorganic/polymer composites could be conveniently fabricated by electrospinning (in air) alcoholic solutions containing both metal alkoxide precursors and PVP.[4c] Under appropriate conditions, the alkoxide precursor could be rapidly hydrolyzed by the moisture in air to generate an amorphous oxide as the liquid jets were accelerated toward the collector. The amorphous oxide could then be transformed into a polycrystalline structure as the PVP matrix was selectively removed by calcining the sample in air at elevated temperatures. If the percentage of the alkoxide precursor was sufficiently high, it was possible to obtain continuous nanofibers made of various polycrystalline metal oxides as uniaxially aligned arrays. Figure 3B shows the SEM image of a parallel array of composite nanofibers that were electrospun from a solution containing 0.15 g of PVP, 0.4 g of titanium tetraisopropoxide, 1 mL of acetic acid, and 4 mL of 2-propanol using a voltage of 7.6 kV. The average diameter of these composite nanofibers was 78 nm. Calcination of the sample at 500 °C led to the formation of continuous nanofibers of polycrystalline titania with their average diameter being reduced to 54 nm (Figure 3C and the inset). The high-magnification SEM image in the inset also indicates that these TiO_2 nanofibers were composed of nanoparticles 10 nm in diameter. Electron diffraction and XRD patterns taken from this sample indicate that these nanoparticles were crystallized in the anatase phase of titania. Figure 3D shows the SEM images of another example: Sb-doped SnO_2 nanofibers that were prepared by electrospinning

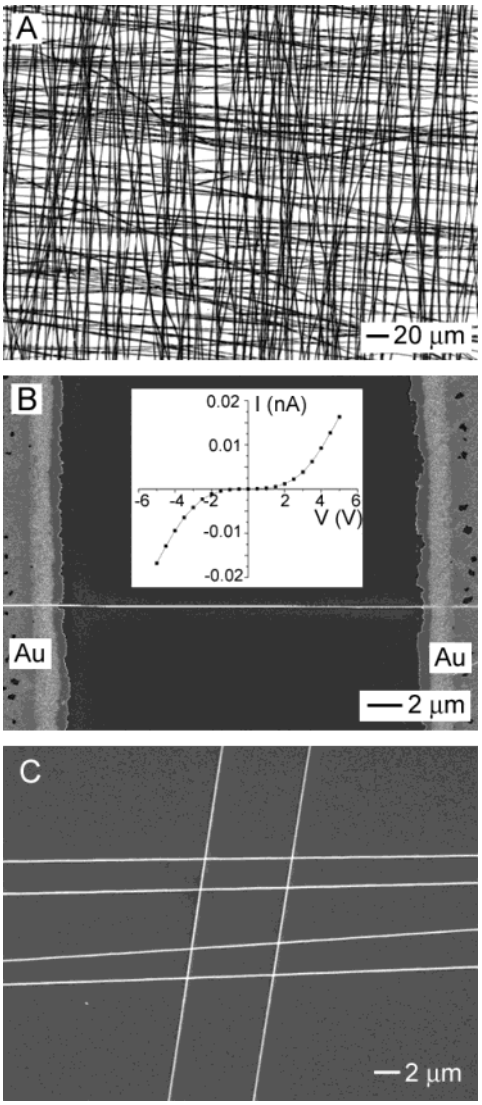

Figure 4. (A) Optical micrograph of a grid (or mesh) formed by stacking two layers of uniaxially aligned nanofibers (with their long axes rotated by 90°). (B, C) SEM images of two simple device structures that were directly fabricated using the electrospinning method: a single SnO_2 nanofiber stretched across two gold electrodes and a 2×4 array of crossbar junctions formed between four SnO_2 nanofibers. The inset in B shows a typical $I-V$ curve measured from an individual Sb-doped SnO_2 nanofiber.

a solution containing 0.15 g of PVP, 0.4 g of tin isopropoxide, 0.04 g of antimony(III) isopropoxide, 0.5 mL of acetic acid, 0.5 mL of acetylacetone, and 4 mL of 2-propanol using a voltage of 7.6 kV, followed by calcination at 500 °C for 3 h. The average diameter of these fibers was 80 nm, and they were composed of nanoparticles 7 nm in diameter. It is worth mentioning that organic functional molecules (e.g., dyes), biomolecules, and nanoparticles (e.g., superparamagnetic iron oxides) could also be easily incorporated into the electrospinning solutions to generate uniaxially aligned nanofibers with desired functionalities.

The uniaxially aligned arrays of nanofibers could be stacked in a layer-by-layer fashion to generate a 3D grid structure. Figure 4A shows the optical micrograph (dark field) of such a mesh that was fabricated by transferring two layers of uniaxially aligned PVP fibers onto the same substrate, with the long axes of their fibers rotated by 90°. In addition to arrays containing large numbers of fibers that often overlapped each other, well-separated nanofibers could be conveniently fabricated using the same setup but with shorter collection times. When the collection times were shorter than 1 s, for example, only a small number of nanofibers were deposited across the gap. These fibers tended to be separated from each other because of repulsive interactions between the residual charges on their surfaces. Because these nanofibers had been physically fixed across the gap, their spatial position and orientation could be easily manipulated by moving around the collector. By taking advantage of light-scattering effects, these nanofibers could also be visualized by the naked eye under the irradiation of an ordinary light source. All of these features make these nanofibers particularly useful as building blocks in fabricating device structures with simple designs. Figure 4B shows the SEM image of an individual Sb-doped SnO_2 nanofiber that was collected on top of a gap and subsequently transferred onto two gold electrodes separated by ~ 20 μm. The inset shows a nonlinear current−voltage ($I-V$) curve measured from this nanofiber, with behavior similar to that of a metal oxide varistor.[13] In addition to its use in conductivity measurements, such a configuration could be further explored to fabricate arrayed chemical sensors. Figure 4C shows another example, where SnO_2 nanofibers were transferred onto the same substrate in two consecutive steps (with the long axes of nanofibers rotated by 90°) to form a 2×4 array of crossbar junctions. By carefully controlling the conditions for electrospinning, this method might provide a simple route to arrays of crossbar junctions with relatively high densities and over large areas.

The ability to electrospin various materials into uniaxially aligned nanofibers opens the door to the exploration of a range of intriguing properties and applications associated with 1D nanostructures. For example, the preferential alignment of nanofibers should lead to the formation of nanostructured materials with highly anisotropic behavior.[14] In one demonstration, it was found that the electrical conductivity of a free-standing thin film consisting of uniaxially aligned carbon nanofibers (Figure 3A) and aligned SnO_2 nanofibers (slightly doped with Sb, Figure 3D) was highly anisotropic. The ratio between the conductivities parallel and perpendicular to the long axis of the nanofiber was ~ 15 for a film containing ~ 900 nanofibers per millimeter (along the direction perpendicular to the long axis). This anisotropic ratio is greater than those of thin films containing aligned carbon nanotubes.[14] Figure 5 shows another demonstration where Rayleigh scattering spectra were recorded from a parallel array of PVP nanofibers to evaluate its performance as an optical polarizer. As predicted by the Maxwell−Garnett model,[15] the attenuation of light is greater for the electric field polarized parallel to the long axis of an infinite cylinder than the component perpendicular to the axis. Our measurements agreed with this prediction in that the incident light with polarization parallel to the long axis could be made extinct by three times as much when compared with the light polarized perpendicular to the long axes of fibers. In addition to polymers, polariza-

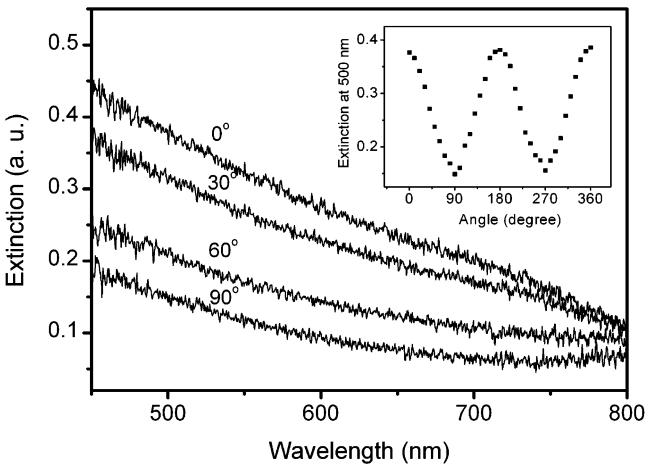

Figure 5. Rayleigh scattering spectra taken from a uniaxially aligned array of PVP nanofibers (~90 nm in diameter) with the polarizer oriented at various angles relative to the longitudinal axes of the nanofibers. The inset shows how the extinction at 500 nm was modulated (as a cosine wave) as a function of the angle between the nanofibers and the polarization.

tion-dependent light scattering was also observed for uniaxially aligned ceramic nanofibers. For all of these systems that exhibit no significant absorption features in the visible region, the extinction recorded at a specific wavelength (in the visible region) exhibited a cosine-like dependence on the polarization angle (Figure 5 inset). The extinction ratio was ~3, and this contrast could be further improved by increasing the packing density of the nanofibers.

In summary, we have demonstrated a simple and versatile method based on electrospinning for generating uniaxially aligned nanofibers made of polymers, ceramics, and composite materials. The uniaxial alignment was achieved by collecting the electrospun nanofibers over a gap formed between two conductive substrates. As a result of electrostatic interactions, the nanofibers were stretched to form a parallel array across the gap. In addition to the materials described in this paper, we have also successfully processed a variety of other ceramics (e.g., Al_2O_3, Fe_2O_3, ZrO_2, $BaTiO_3$, and $NiFe_2O_4$) into well-aligned nanofibers. It is believed that this method could be extended to cover functional materials (e.g., electrical, magnetic, ferroelectric, ferromagnetic, and structural mechanical) where an anisotropic alignment of active components is expected to bring in new features and applications.

Acknowledgment. This work has been supported in part by an AFOSR-DURINT subcontract from SUNY Buffalo, a Career Award from the NSF (DMR-9983893), and a research Fellowship from the David and Lucile Packard Foundation. Y.X. is a Camille Dreyfus Teacher Scholar (2002) and an Alfred P. Sloan Research Fellow (2000). We thank Dr. D. Qin of the Nanotech User Facility for SEM analysis.

References

(1) Reneker, D. H.; Chun, I. *Nanotechnology* **1996**, *7*, 216.
(2) (a) Reneker, D. H.; Yarin, A. L.; Fong, H.; Koombhongse, S. *J. Appl. Phys.* **2000**, *87*, 4531. (b) Shin, Y. M.; Hohman, M. M.; Brenner, M. P.; Rutledge, G. C. *Polymer* **2001**, *42*, 9955.
(3) (a) Srinivasan, G.; Reneker, D. H. *Polym. Int.* **1995**, *36*, 195. (b) Ohgo, K.; Zhao, C.; Kobayashi, M.; Asakura, T. *Polymer* **2003**, *44*, 841. (c) MacDiarmid, A. G.; Jones, W. E.; Norris, I. D.; Gao, J.; Johnson, A. T.; Pinto, N. J.; Hone, J.; Han, B.; Ko, F. K.; Okuzaki, H.; Llaguno, M. *Synth. Met.* **2001**, *119*, 27. (d) Fong, H.; Reneker, D. H. *J. Polym. Sci., Part B* **1999**, *37*, 3488. (e) Jin, H.-J.; Fridrikh, S. V.; Rutledge, G. C.; Kaplan, D. L. *Biomacromolecules* **2002**, *3*, 1233. (f) Bognitzki, M.; Czado, W.; Frese, T.; Schaper, A.; Hellwig, M.; Steinhart, M.; Greiner, A.; Wendorff, J. H. *Adv. Mater.* **2001**, *13*, 70.
(4) (a) Larsen, G.; Velarde-Ortiz, R.; Minchow, K.; Barrero, A.; Loscertales, I. G. *J. Am. Chem. Soc.* **2003**, *125*, 1154. (b) Dai, H.; Gong, J.; Kim, H.; Lee, D. *Nanotechnology* **2002**, *13*, 674. (c) Li, D.; Xia, Y. *Nano Lett.* **2003**, *3*, 555.
(5) (a) Pawlowski, K. J.; Belvin, H. L.; Raney, D. L.; Su, J.; Harrison, J. S.; Siochi, E. J. *Polymer* **2003**, *44*, 1309. (b) Dzenis, Y.; Wen, Y. *Mater. Res. Soc. Symp. Proc.* **2002**, *702*, 173. (c) Gibson, P.; Schreuder-Gibson, H.; Rivin, D. *Colloids Surf., A* **2001**, *187*−*188*, 469. (d) Wang, X.; Drew, C.; Lee, S.-H.; Senecal, K. J.; Kumar, J.; Samuelson, L. A. *Nano Lett.* **2002**, *2*, 1273. (e) Wang, Y.; Hsieh, Y.-L. *Polym. Prepr.* **2003**, *44*, 1212. (f) Wnek, G. E.; Carr, M. E.; Simpson, D. G.; Bowlin, G. L. *Nano Lett.* **2003**, *3*, 213.
(6) (a) Kovtyukhova, N. I.; Mallouk, T. E. *Chem.*—*Eur. J.* **2002**, *8*, 4354. (b) Huang, Y.; Duan, X.; Wei, Q.; Lieber, C. M. *Science* **2001**, *291*, 630. (c) Favier, F.; Walter, E. C.; Zach, M. P.; Benter, T.; Penner, R. M. *Science* **2001**, *293*, 2227. (d) Melosh, N. A.; Boukai, A.; Diana, F.; Gerardot, B.; Badolato, A.; Petroff, P. M.; Heath, J. R. *Science* **2003**, *300*, 112. (e) Kim, F.; Kwan, S.; Akana, J.; Yang, P. *J. Am. Chem. Soc.* **2001**, *123*, 4360.
(7) Doshi, J.; Reneker, D. H. *J. Electrost.* **1995**, *35*, 151.
(8) (a) Theron, A.; Zussman, E.; Yarin, A. L. *Nanotechnology* **2001**, *12*, 384. (b) Zussman, E.; Theron, A.; Yarin, A. L. *Appl. Phys. Lett.* **2003**, *82*, 973.
(9) Deitzel, J. M.; Kleinmeyer, J. D.; Hirvonen, J. K.; Beck Tan, N. C. *Polymer* **2001**, *42*, 8163.
(10) Fong, H.; Liu, W. D.; Wang, C. S.; Vaia, R. A. *Polymer* **2002**, *43*, 775.
(11) Dersch, R.; Liu, T.; Schaper, A. K.; Greiner, A.; Wendorff, J. H. *J. Polym. Sci., Part A* **2003**, *41*, 545.
(12) Chun, I.; Reneker, D. H.; Fong, H.; Fang, X. Y.; Dietzel, J.; Tan, N. B.; Kearns, K. *J. Adv. Mater.* **1999**, *31*, 36.
(13) Levinson, L. M.; Philipp, H. R. In *Ceramic Materials for Electronics*; Buchanan, R. C., Ed.; Marcel Dekker: New York, 1991; pp 349−377.
(14) de Heer, W. A.; Bacsa, W. S.; Chatelain, A.; Gerfin, T.; Humphrey-baker, R.; Forro, L.; Ugarte, D. *Science* **1995**, *268*, 845.
(15) (a) Rogers, J. A.; Paul, K. E.; Jackman, R. J.; Whitesides, G. M. *Appl. Phys. Lett.* **1997**, *70*, 2658. (b) Aspnes, D. E. *Thin Solid Films* **1982**, *89*, 249.

NL0344256